Geophys. J. Int. (2005) **163,** 372–384 doi: 10.1111/j.1365-246X.2005.02722.x

A model for *P*-wave attenuation and dispersion in a porous medium permeated by aligned fractures

Miroslav Brajanovski,[1] Boris Gurevich[1,2] and Michael Schoenberg[3]

[1]*Department of Exploration Geophysics, Curtin University of Technology, GPO Box* U1987, *Perth, Western Australia* 6845, *Australia.*
E-mail: Boris.Gurevich@geophy.curtin.edu.au
[2]*CSIRO Division of Petroleum Resources, Perth, Western Australia, Australia*
[3]5 *Mountain Road, W. Redding, CT* 06896, *USA*

Accepted 2005 June 24. Received 2005 January 27; in original form 2004 May 19

SUMMARY

Fractures in a porous rock can be modelled as very thin and highly porous layers in a porous background. First, a dispersion equation for a P wave propagating in periodically layered poroelastic medium is obtained using propagator matrix approach applied to Biot equations of poroelasticity with periodic coefficients. Then in the limit of low stiffness and thickness this dispersion equation yields an expression for the effective P-wave modulus of the fractured porous material. When both pores and fractures are dry, this material is equivalent to a transversely isotropic elastic porous material with linear–slip interfaces. When saturated with a liquid this material exhibits significant attenuation and velocity dispersion due to wave-induced fluid flow between pores and fractures. In the low-frequency limit the material properties are equal to those obtained by anisotropic Gassmann (or Brown–Korringa) theory applied to a porous material with linear-slip interfaces. At low frequencies inverse quality factor scales with the first power of frequency ω. At high frequencies the effective elastic properties are equal to those for isolated fluid-filled fractures in a solid (non-porous) background, and inverse quality factor scales with $\omega^{-1/2}$. The magnitude of both attenuation and dispersion strongly depends on both the degree of fracturing and background porosity of the medium. The characteristic frequency of the attenuation and dispersion depends on the background permeability, fluid viscosity, as well as fracture density and spacing.

Key words: anisotropy, attenuation, dispersion, porous media, wave propagation.

1 INTRODUCTION

Naturally fractured reservoirs have attracted an increased interest from exploration and production geophysics in recent years. In many instances, natural fractures control the permeability of the reservoir, and hence the ability to find and characterize fractured areas of the reservoir represents a major challenge for seismic investigations.

One of the main issues in the characterization of any reservoir is the ability to predict the effect of fluid on its elastic properties. For isotropic porous reservoirs this effect is expressed through Gassmann equations, which provide explicit analytical expressions for the effective elastic moduli of a fluid-saturated rock as functions of the porosity, the elastic moduli of the dry skeleton, bulk modulus of the solid grain material and the bulk modulus of the pore fluid. In fractured and porous reservoirs the effect of the saturating fluid on elastic properties becomes more complex, as the fluid affects elastic anisotropy of the rock and may also cause significant frequency-dependent attenuation and dispersion (Thomsen 1995; Hudson *et al.* 1996, 2001; Tod 2001). Recent analysis of field observations shows that these effects may be significant (Maultzsch *et al.* 2003).

Theoretical models of attenuation and dispersion due to wave-induced fluid flow between pores in fractures have recently been developed by Hudson *et al.* (1996) and Chapman (2003). These models have been developed for a sparse concentration of penny-shaped cracks in a porous matrix. A more general approach to modelling fractures in porous media can be based on Biot's theory of poroelasticity (Biot 1962). In the context of Biot's theory fractures can be modelled as highly compliant heterogeneities, thus allowing applications of the methods developed to study wave propagation in heterogeneous poroelastic materials (Norris 1993; Gurevich & Lopatnikov 1995; Pride *et al.* 2004).

The aim of this paper is to develop a theoretical model for elastic wave attenuation and dispersion caused by wave-induced fluid flow between pores in fractures. To this end, by analogy with the linear-slip approach for elastic fractured media (Schoenberg 1980), we model fractures as highly porous thin layers in a porous background. By assuming that the porous medium is permeated by a periodic sequence of such fractures, and using the results of Norris (1993) for frequency-dependent effective moduli of a periodically layered poroelastic medium, we will derive the elastic properties of the system of pores and fractures. In Section 2 we describe the geometry of the system and introduce the necessary notation. In Section 3 we define the elastic properties of the dry medium in terms of the linear-slip model. In Section 4 we derive the closed-form expression for the P-wave modulus of the porous fractured system saturated with a viscous fluid. In Section 5 this expression is analysed in the limits of low and high frequencies. Numerical examples are shown in Section 6.

2 GEOMETRY OF THE MODEL

We model a porous medium with aligned fractures as a periodic (with spatial period H) horizontally stratified system of alternating, relatively thick, layers of a finite-porosity background material and relatively thin layers of a high-porosity material composing the fractures, see Fig. 1. The background material is specified by porosity ϕ_b, permeability κ_b, dry (drained) bulk modulus K_b, shear modulus μ_b and thickness fraction h_b so that the thickness of a background layer is $h_b H$, where h_b is assumed to be close to 1. The material comprising the fractures is specified by porosity ϕ_c, permeability κ_c, dry bulk modulus K_c, shear modulus μ_c and thickness fraction $h_c = 1 - h_b \ll 1$ so that the thickness of a fracture is $h_c H$. Both background and fractures are assumed to be made of the same isotropic grain material with bulk modulus K_g, shear modulus μ_g and density ρ_g, and to be saturated with the same fluid with bulk modulus K_f, density ρ_f and dynamic viscosity η. Our aim is to compute frequency-dependent elastic wave velocities in such a system of layers in the limit $h_c \to 0$ and $\phi_c \to 1$.

Elastic waves in such periodically layered and porous medium can be described by Biot's equations of poroelasticity (Biot 1962) with spatially periodic and piecewise constant coefficients. Biot's equations of poroelasticity with periodically varying coefficients have been analysed by Norris (1993). The results of Norris (1993) can be used to relate overall elastic properties of the layered system to the properties of the background and fracture media. The properties of the fractured medium can then be established by taking the small fracture thickness limit $h_c \to 0$. In this limit the contribution of the fractures can only be significant if at the same time $K_c \to 0$, which is always the case when $\phi_c \to 1$. To understand the relationship between different fracture parameters and to relate those parameters to the commonly used fracture properties, we first consider the dry fractured medium.

3 DRY FRACTURED POROUS ROCK: CONNECTION WITH LINEAR–SLIP THEORY

Since our aim is to study the effects of wave-induced fluid flow, we assume that the solid frame is ideally elastic. Therefore, when the stratified medium is dry ($K_f = \rho_f = 0$), the layers behave as ideal elastic isotropic solids. Note that the Lamé parameter λ is such that $\lambda + 2\mu = K + 4\mu/3 \equiv L$ and it is convenient to define the parameter

$$\gamma \equiv \frac{\mu}{L}. \tag{1}$$

Physically, γ is the square of the ratio of shear wave speed to compressional wave speed, and as such it is always between 0 and 3/4 (and for positive Poisson ratio media, between 0 and 1/2). In the long wavelength limit, the system of horizontal layers perpendicular to x_3 axis is then

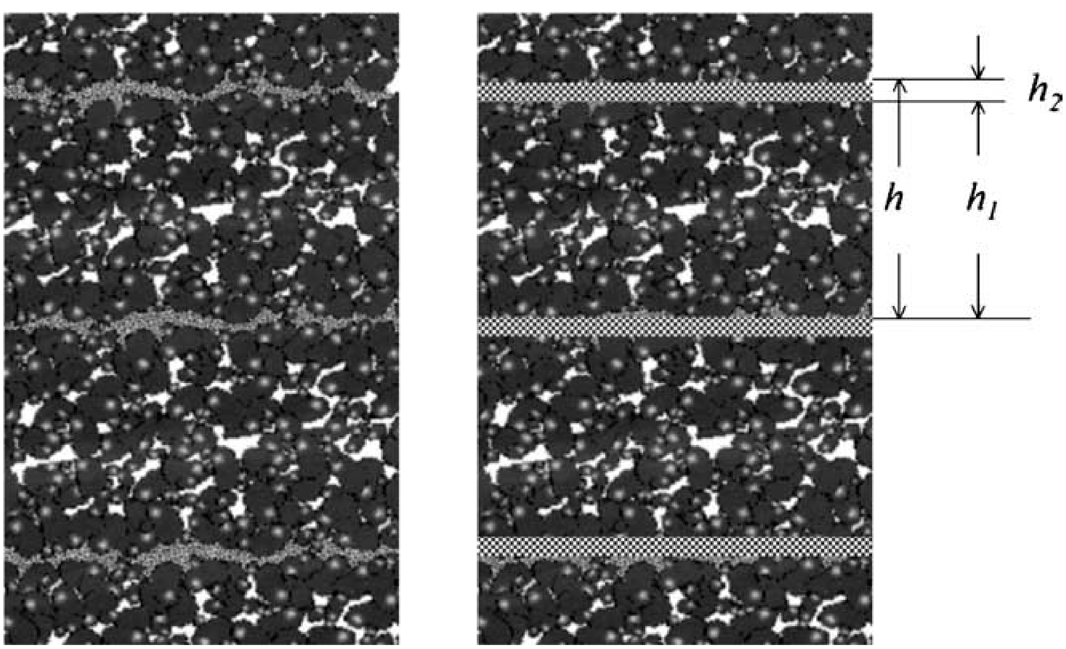

Figure 1. Porous fractured medium and its model representation.

equivalent to a transversely isotropic elastic solid with stiffness matrix

$$
\mathbf{c}^{\mathrm{dry}} = \begin{pmatrix}
\frac{(1-2\langle\gamma\rangle)^2}{\langle 1/L\rangle} + 4\langle\mu\rangle - 4\langle\gamma\mu\rangle & \frac{(1-2\langle\gamma\rangle)^2}{\langle 1/L\rangle} + 2\langle\mu\rangle - 4\langle\gamma\mu\rangle & \frac{1-2\langle\gamma\rangle}{\langle 1/L\rangle} & 0 & 0 & 0 \\
\frac{(1-2\langle\gamma\rangle)^2}{\langle 1/L\rangle} + 2\langle\mu\rangle - 4\langle\gamma\mu\rangle & \frac{(1-2\langle\gamma\rangle)^2}{\langle 1/L\rangle} + 4\langle\mu\rangle - 4\langle\gamma\mu\rangle & \frac{1-2\langle\gamma\rangle}{\langle 1/L\rangle} & 0 & 0 & 0 \\
\frac{1-2\langle\gamma\rangle}{\langle 1/L\rangle} & \frac{1-2\langle\gamma\rangle}{\langle 1/L\rangle} & \frac{1}{\langle 1/L\rangle} & 0 & 0 & 0 \\
0 & 0 & 0 & \frac{1}{\langle 1/\mu\rangle} & 0 & 0 \\
0 & 0 & 0 & 0 & \frac{1}{\langle 1/\mu\rangle} & 0 \\
0 & 0 & 0 & 0 & 0 & \langle\mu\rangle
\end{pmatrix}, \tag{2}
$$

where brackets $\langle\cdot\rangle$ indicate the thickness weighted average of the enclosed property, that is, $\langle q\rangle = h_b q_b + h_c q_c = (1-h_c)q_b + h_c q_c$. Inversion of stiffness matrix $\mathbf{c}^{\mathrm{dry}}$ yields the compliance matrix $\mathbf{s}^{\mathrm{dry}} = (\mathbf{c}^{\mathrm{dry}})^{-1}$

$$
\mathbf{s}^{\mathrm{dry}} = \begin{pmatrix}
\frac{1-\langle\gamma\mu\rangle/\langle\mu\rangle}{3\langle\mu\rangle-4\langle\gamma\mu\rangle} & -\frac{1-2\langle\gamma\mu\rangle/\langle\mu\rangle}{2(3\langle\mu\rangle-4\langle\gamma\mu\rangle)} & -\frac{1-2\langle\gamma\rangle}{2(3\langle\mu\rangle-4\langle\gamma\mu\rangle)} & 0 & 0 & 0 \\
-\frac{1-2\langle\gamma\mu\rangle/\langle\mu\rangle}{2(3\langle\mu\rangle-4\langle\gamma\mu\rangle)} & \frac{1-\langle\gamma\mu\rangle/\langle\mu\rangle}{3\langle\mu\rangle-4\langle\gamma\mu\rangle} & -\frac{1-2\langle\gamma\rangle}{2(3\langle\mu\rangle-4\langle\gamma\mu\rangle)} & 0 & 0 & 0 \\
-\frac{1-2\langle\gamma\rangle}{2(3\langle\mu\rangle-4\langle\gamma\mu\rangle)} & -\frac{1-2\langle\gamma\rangle}{2(3\langle\mu\rangle-4\langle\gamma\mu\rangle)} & \left\langle\frac{1}{L}\right\rangle + \frac{(1-2\langle\gamma\rangle)^2}{3\langle\mu\rangle-4\langle\gamma\mu\rangle} & 0 & 0 & 0 \\
0 & 0 & 0 & \left\langle\frac{1}{\mu}\right\rangle & 0 & 0 \\
0 & 0 & 0 & 0 & \left\langle\frac{1}{\mu}\right\rangle & 0 \\
0 & 0 & 0 & 0 & 0 & \frac{1}{\langle\mu\rangle}
\end{pmatrix}. \tag{3}
$$

Then taking the limit $h_c \to 0$ while $\mu_c, L_c \to 0$ (with the ratio between them, γ_c, remaining constant) gives the following results:

$$
\langle\mu\rangle \to \mu_b\,, \quad \langle\gamma\rangle \to \gamma_b\,, \qquad \langle\gamma\mu\rangle \to \gamma_b\mu_b\,,
$$
$$
\left\langle\frac{1}{\mu}\right\rangle \to \frac{1}{\mu_b} + \lim_{h_c\to 0}\frac{h_c}{\mu_c}\,, \qquad \left\langle\frac{1}{L}\right\rangle \to \frac{1}{L_b} + \lim_{h_c\to 0}\frac{h_c}{L_c}. \tag{4}
$$

Substitution of these results into eq. (3) while noting that E_b (the dynamic Young's modulus) and ν_b (the dynamic Poisson's ratio) of the background medium are given, in terms of μ_b and γ_b, by

$$
E_b = \frac{3-4\gamma_b}{1-\gamma_b}\mu_b, \quad \nu_b = \frac{\frac{1}{2}-\gamma_b}{1-\gamma_b}, \tag{5}
$$

yields the compliance matrix of the dry fractured porous medium,

$$
\mathbf{s}^{\mathrm{dry}} = \begin{pmatrix}
\frac{1}{E_b} & -\frac{\nu_b}{E_b} & -\frac{\nu_b}{E_b} & 0 & 0 & 0 \\
-\frac{\nu_b}{E_b} & \frac{1}{E_b} & -\frac{\nu_b}{E_b} & 0 & 0 & 0 \\
-\frac{\nu_b}{E_b} & -\frac{\nu_b}{E_b} & \frac{1}{E_b} & 0 & 0 & 0 \\
0 & 0 & 0 & \frac{1}{\mu_b} & 0 & 0 \\
0 & 0 & 0 & 0 & \frac{1}{\mu_b} & 0 \\
0 & 0 & 0 & 0 & 0 & \frac{1}{\mu_b}
\end{pmatrix} + \lim_{h_c\to 0}\begin{pmatrix}
0 & 0 & 0 & 0 & 0 & 0 \\
0 & 0 & 0 & 0 & 0 & 0 \\
0 & 0 & \frac{h_c}{L_c} & 0 & 0 & 0 \\
0 & 0 & 0 & \frac{h_c}{\mu_c} & 0 & 0 \\
0 & 0 & 0 & 0 & \frac{h_c}{\mu_c} & 0 \\
0 & 0 & 0 & 0 & 0 & 0
\end{pmatrix} \tag{6}
$$

or

$$
\mathbf{s}^{\mathrm{dry}} \equiv \mathbf{s}_b^{\mathrm{dry}} + \mathbf{s}_c^{\mathrm{dry}}. \tag{7}
$$

The first matrix, $\mathbf{s}_b^{\mathrm{dry}}$, is compliance matrix for the dry background material, and the second matrix, $\mathbf{s}_c^{\mathrm{dry}}$, is the excess compliance due to the dry fractures.

Eq. (6) is equivalent to the equation for the compliance matrix of a fractured medium as given by linear-slip deformation theory (Schoenberg & Douma 1988; Schoenberg & Sayers 1995), which stipulates that the compliance of an elastic medium with aligned rotationally symmetric (on average) fractures can be written as a sum of the compliance matrix of the background plus an excess compliance given by

$$
\mathbf{s}_e = \begin{pmatrix}
0 & 0 & 0 & 0 & 0 & 0 \\
0 & 0 & 0 & 0 & 0 & 0 \\
0 & 0 & Z_N & 0 & 0 & 0 \\
0 & 0 & 0 & Z_T & 0 & 0 \\
0 & 0 & 0 & 0 & Z_T & 0 \\
0 & 0 & 0 & 0 & 0 & 0
\end{pmatrix}, \tag{8}
$$

where Z_N and Z_T are called excess normal and tangential compliances, respectively. Equivalence between $\mathbf{s}_c^{\mathrm{dry}}$ and $\mathbf{s}_e$ can be established by assuming that the shear modulus μ_c and the longitudinal modulus $K_c + 4\mu_c/3$ are $\mathcal{O}(h_c)$ as $h_c \to 0$, and by defining

$$\lim_{h_c \to 0} \frac{h_c}{L_c} \equiv Z_N, \quad \lim_{h_c \to 0} \frac{h_c}{\mu_c} \equiv Z_T. \tag{9}$$

Eq. (9) mean that the fractures in the dry porous background are modelled as very thin and very soft porous layers. Using eq. (9), we can relate the solutions of Biot's equations of poroelasticity for the fluid-saturated medium to the excess fracture compliances Z_N and Z_T (Schoenberg & Sayers 1995). These excess compliances can in turn be related to the fracture density and aspect ratio for penny-shaped cracks (Schoenberg & Douma 1988). Note that Schoenberg & Sayers (1995) obtained the result $\mathbf{s}^{\mathrm{dry}} = \mathbf{s}_b^{\mathrm{dry}} + \mathbf{s}_e$ directly from a compliance formulation based on linear slip for aligned fractures without going through equivalent medium theory for layers in the stiffness domain.

4 FLUID-SATURATED FRACTURED POROUS MEDIUM

Whereas the dry rock in our model is elastic, the fluid-saturated rock may exhibit frequency-dependent attenuation and velocity dispersion due to the wave-induced fluid flow between pores and fractures. Elastic waves in such a periodically layered and porous medium can be described by Biot's equations of poroelasticity (Biot 1962) with periodic and piecewise constant coefficients. Let C_j denote the fluid-saturated P-wave modulus of layer j given by Gassmann's equation (Gassmann 1951; White 1983):

$$C_j = L_j + \alpha_j^2 M_j, \tag{10}$$

where

$$\alpha_j = 1 - \frac{K_j}{K_g}, \tag{11}$$

is Biot's effective stress coefficient and M is pore space modulus

$$\frac{1}{M_j} = \frac{\alpha_j - \phi_j}{K_g} + \frac{\phi_j}{K_f}. \tag{12}$$

White *et al.* (1975) and Norris (1993) showed that for frequencies much smaller than Biot's characteristic frequency $\omega_B = \eta\phi/\kappa\rho_f$, and also much smaller than the resonant frequency of the layering $\omega_R = V_p/H$, the compressional wave modulus c_{33}^{sat} of a periodically layered fluid-saturated porous medium composed of two constituents, b and c can be written in the form

$$\frac{1}{c_{33}^{\mathrm{sat}}} = \left\langle \frac{1}{C} \right\rangle + \frac{2}{\sqrt{i\omega\eta}H} \; \frac{\left(\frac{\alpha_b M_b}{C_b} - \frac{\alpha_c M_c}{C_c}\right)^2}{\sqrt{\frac{M_b L_b}{C_b \kappa_b}} \cot\left(\sqrt{\frac{i\omega\eta C_b}{\kappa_b M_b L_b}} \frac{h_b H}{2}\right) + \sqrt{\frac{M_c L_c}{C_c \kappa_c}} \cot\left(\sqrt{\frac{i\omega\eta C_c}{\kappa_c M_c L_c}} \frac{h_c H}{2}\right)}. \tag{13}$$

The derivation of eq. (13) is reproduced in Appendix 1 using propagator matrix approach. Physically, the quantity $\kappa_b M_b L_b/\eta C_b \equiv D_b$ in the denominator of the right hand side of eq. (13) is the diffusion coefficient appearing in the dispersion relation for Biot's slow wave in the background medium.

The effective P-wave modulus of the fractured porous medium can be obtained by taking the limit $h_c \to 0$ (and setting h_b to 1) in eq. (13), while at the same time assuming L_c and μ_c (and hence K_c) are $\mathcal{O}(h_c)$ as was done for the dry fractures. Note that this implies that $\alpha_c \to 1$ and

$$\lim_{h_c \to 0} C_c = \lim_{h_c \to 0} M_c = \frac{1}{\frac{1-\phi_c}{K_g} + \frac{\phi_c}{K_f}}\ , \tag{14}$$

a finite value (close to K_f/ϕ_c if ϕ_c is not small and $K_g \gg K_f$), as $h_c \to 0$. From eq. (14) we see $M_c/C_c \to 1$ so that $M_c L_c/C_c \to L_c = \mathcal{O}(h_c)$. Thus, as $h_c \to 0$, the argument of the trigonometric cotangent function relating to the fracture material is $\mathcal{O}(h_c^{1/2})$. Since $\cot x \simeq 1/x$ for any complex x with $|x| \to 0$, in the limit $h_c \to 0$ eq. (13) yields

$$\frac{1}{c_{33}^{\mathrm{sat}}} = \frac{1}{C_b} + \frac{\left(\frac{\alpha_b M_b}{C_b} - 1\right)^2}{\frac{M_b}{C_b}\sqrt{\frac{i\omega}{D_b}}\frac{H}{2}\cot\left(\sqrt{\frac{i\omega}{D_b}}\frac{H}{2}\right) + \frac{1}{Z_N}}. \tag{15}$$

Here we have used the definition of Z_N from eq. (9). Note that $\sqrt{D_b/\omega}$ in the argument of the cotangent corresponds to the fluid diffusion length in the background medium.

Eq. (15) is the central result of this paper. It gives the P-wave modulus for waves propagating normal to fractures as a function of frequency, background properties and normal fracture compliance Z_N. The corresponding P-wave velocity along the symmetry axis x_3 is given by

$$V_{p3} = \sqrt{\frac{c_{33}^{\mathrm{sat}}}{\rho_b}}, \tag{16}$$

where $\rho_b = \rho_g(1 - \phi_b) + \rho_f \phi_b$ is mass density of the fluid-saturated background material. This velocity is complex and frequency-dependent, indicating the presence of velocity dispersion and frequency-dependent attenuation.

The results presented in this section are valid for the same frequency range as the original eq. (13), that is, for frequencies that satisfy the conditions $\omega \ll \omega_B$, which implies that the frequencies are sufficiently low so that the fluid flow in the pore channels is Poiseuille flow, and $\omega \ll \omega_R$, which means that the effective medium approximation is still valid and implies that without the fluid flow the effective elastic moduli of the system would be given by Backus averaging.

It is important to note that according to eq. (13) within the conditions $\omega \ll \min(\omega_B, \omega_R)$, the wave velocity and attenuation will be frequency-dependent due to the fluid flow between the fractures and the background (or between different layers). Consequently, under these conditions we still can define low and high frequencies with respect to fluid flow. Low frequencies are those when pressure has enough time to equilibrate between layers within the wave cycle. This occurs when the diffusion length $\sqrt{D_b/\omega}$ (or wavelength of Biot's slow wave) is much larger than the spatial period H, that is,

$$\omega \ll D_b/H^2. \tag{17}$$

High frequencies are those much higher than D_b/H^2 but still smaller than both ω_B and ω_R. Below we analyse these results by examining limiting cases of low and high frequencies in the range described above.

5 LIMITING MODULI

5.1 Low frequencies

In the low-frequency limit $\omega \to 0$, the cotangent function in eq. (15) can be replaced by the inverse of its argument. The expression for c_{33}^{sat} reduces to

$$\frac{1}{c_{33_0}^{\mathrm{sat}}} = \frac{1}{C_b} + \frac{\left(\frac{\alpha_b M_b}{C_b} - 1\right)^2}{\frac{M_b L_b}{C_b} + \frac{1}{Z_N}} = \frac{1}{C_b}\left[1 + \frac{Z_N(\alpha_b M_b - C_b)^2}{C_b\left(1 + \frac{M_b L_b}{C_b} Z_N\right)}\right]. \tag{18}$$

Eq. (18) provides an expression for the P-wave modulus for waves propagating normal to the fractures for low frequencies, that is, for frequencies low enough to allow equilibration of the fluid pressure p between fractures and the background during the period of the wave.

Norris (1993) and Gelinsky & Shapiro (1997) investigated this specific situation by assuming pressure p is constant, directly in Biot's equations, without referring to the frequency-dependent solution, and derived the following expressions for low-frequency moduli of the finely layered porous continuum:

$$c_{33_0}^{\mathrm{sat}} = \left\langle \frac{1 - \alpha B}{L} \right\rangle^{-1}, \tag{19}$$

$$c_{13_0}^{\mathrm{sat}} = c_{33_0}^{\mathrm{sat}} \left\langle \frac{\lambda + \alpha A}{L} \right\rangle, \tag{20}$$

$$c_{11_0}^{\mathrm{sat}} = \frac{\left(c_{13_0}^{\mathrm{sat}}\right)^2}{c_{33_0}^{\mathrm{sat}}} + \left\langle \frac{2\mu\,(\lambda + \alpha A)}{L} \right\rangle + \langle 2\mu \rangle\,, \tag{21}$$

where:

$$A = \left\langle \frac{1}{M} + \frac{\alpha^2}{L} \right\rangle^{-1} \left\langle 2\mu \frac{\alpha}{L} \right\rangle, \quad B = \left\langle \frac{1}{M} + \frac{\alpha^2}{L} \right\rangle^{-1} \left\langle \frac{\alpha}{L} \right\rangle. \tag{22}$$

Shear stiffnesses are unaffected by the fluid so that

$$c_{55_0}^{\mathrm{sat}} = c_{55_0}^{\mathrm{dry}} = \left\langle \frac{1}{\mu} \right\rangle^{-1}, \qquad c_{66_0}^{\mathrm{sat}} = c_{66_0}^{\mathrm{dry}} = \langle \mu \rangle\,. \tag{23}$$

Eq. (19) can be rewritten as

$$\frac{1}{c_{33_0}^{\mathrm{sat}}} = \left\langle \frac{1}{L} \right\rangle - \frac{\left\langle \frac{\alpha}{L} \right\rangle^2}{\left\langle \frac{C}{ML} \right\rangle}. \tag{24}$$

For a system of alternating layers of types b and c, eq. (24) becomes

$$\frac{1}{c_{33_0}^{\mathrm{sat}}} = \frac{h_b}{C_b}\frac{L_b + \alpha_b^2 M_b}{L_b} + \frac{h_c}{C_c}\frac{L_c + \alpha_c^2 M_c}{L_c} - \frac{\left(\frac{\alpha_b h_b}{L_b} + \frac{\alpha_c h_c}{L_c}\right)^2}{\frac{C_b h_b}{L_b M_b} + \frac{C_c h_c}{L_c M_c}}. \tag{25}$$

After a simple rearrangement, we obtain

$$\frac{1}{c_{33_0}^{\mathrm{sat}}} = \left(\frac{h_b}{C_b} + \frac{h_c}{C_c}\right) + \frac{\left(\frac{\alpha_b M_b}{C_b} - \frac{\alpha_c M_c}{C_c}\right)^2}{\frac{M_b L_b}{C_b h_b} + \frac{M_c L_c}{C_c h_c}}$$

which is precisely the zero-frequency limit of eq. (13).

Introducing parameter γ in eqs (20) and (21), for the moduli $c^{\mathrm{sat}}_{13_0}$ and $c^{\mathrm{sat}}_{11_0}$ we find:

$$c^{\mathrm{sat}}_{13_0} = c^{\mathrm{sat}}_{33_0}\left(1 - 2\langle\gamma\rangle + 2\left\langle\frac{\alpha}{L}\right\rangle\frac{\langle\alpha\gamma\rangle}{\left\langle\frac{C}{ML}\right\rangle}\right), \quad c^{\mathrm{sat}}_{11_0} = \frac{\left(c^{\mathrm{sat}}_{13_0}\right)^2}{c^{\mathrm{sat}}_{33_0}} + 4\left(\langle\mu\rangle - \langle\gamma\mu\rangle + \frac{\langle\alpha\gamma\rangle^2}{\left\langle\frac{C}{ML}\right\rangle}\right), \tag{26}$$

where

$$\left\langle\frac{C}{ML}\right\rangle = \left\langle\frac{1}{M} + \frac{\alpha^2}{L}\right\rangle = \frac{\langle\alpha\rangle}{K_g} + \left(\frac{1}{K_f} - \frac{1}{K_g}\right)\langle\phi\rangle + \left\langle\frac{\alpha^2}{L}\right\rangle. \tag{27}$$

Using the parameter γ defined in eq. (11) yields

$$\alpha_j = 1 - \frac{\left(1 - \frac{4\gamma_j}{3}\right)L_j}{K_g}. \tag{28}$$

Therefore,

$$\langle\alpha\rangle = 1 - \frac{\langle L\rangle - \frac{4}{3}\langle\mu\rangle}{K_g}, \quad \langle\alpha\gamma\rangle = \langle\gamma\rangle - \frac{\langle\mu\rangle - \frac{4}{3}\langle\gamma\mu\rangle}{K_g}, \quad \left\langle\frac{\alpha}{L}\right\rangle = \left\langle\frac{1}{L}\right\rangle - \frac{1 - \frac{4}{3}\langle\gamma\rangle}{K_g}, \tag{29}$$

and

$$\left\langle\frac{\alpha^2}{L}\right\rangle = \left\langle\frac{1}{L}\right\rangle - 2\frac{1 - \frac{4}{3}\langle\gamma\rangle}{K_g} + \frac{\left\langle\frac{1}{L}\right\rangle - \frac{8}{3}\langle\mu\rangle + \frac{16}{9}\langle\gamma\mu\rangle}{K_g^2}. \tag{30}$$

As with the frequency-dependent P-wave modulus, the low-frequency stiffnesses for the fractured medium can be obtained by taking the small thickness ratio limit $h_c \to 0$. Remembering that L_c and μ_c are required to be $\mathcal{O}(h_c)$, we can write

$$\langle\alpha\rangle \to \alpha_b, \quad \langle\alpha\gamma\rangle \to \alpha_b\gamma_b, \quad \left\langle\frac{\alpha}{L}\right\rangle \to \frac{\alpha_b}{L_b} + Z_N, \quad \left\langle\frac{\alpha^2}{L}\right\rangle \to \frac{\alpha_b^2}{L_b} + Z_N, \tag{31}$$

so that

$$\left\langle\frac{C}{ML}\right\rangle \to \frac{C_b}{L_b M_b} + Z_N. \tag{32}$$

Then eq. (24) gives,

$$\begin{aligned}\frac{1}{c^{\mathrm{sat}}_{33_0}} &= \frac{1}{L_b} + Z_N - \frac{\left(\frac{\alpha_b}{L_b} + Z_N\right)^2}{\frac{C_b}{L_b M_b} + Z_N} = \frac{1}{C_b} + \frac{\alpha_b^2 M_b}{L_b C_b} + Z_N - \frac{\left(\frac{\alpha_b}{L_b} + Z_N\right)^2}{\frac{C_b}{L_b M_b} + Z_N} = \\ &= \frac{1}{C_b} + \frac{Z_N\left(\frac{\alpha_b M_b}{C_b} - 1\right)^2}{1 + Z_N\frac{M_b L_b}{C_b}} = \frac{1}{C_b}\left[1 + \frac{Z_N(\alpha_b M_b - C_b)^2}{C_b\left(1 + Z_N\frac{M_b L_b}{C_b}\right)}\right],\end{aligned} \tag{33}$$

which is identical to eq. (18), as expected.

Taking into account that $(M_b/C_b)(1 + Z_N M_b L_b/C_b) \equiv \alpha_b^2 + L_b/M_b + Z_N L_b$ the small thickness ratio limit $h_c \to 0$ in the first and second of eq. (26) gives

$$\begin{aligned}c^{\mathrm{sat}}_{13_0} &= c^{\mathrm{sat}}_{33_0}\left[1 - 2\gamma_b + 2\alpha_b\gamma_b\frac{M_b}{C_b}\frac{\alpha_b + Z_N L_b}{1 + Z_N\frac{M_b L_b}{C_b}}\right], \\ c^{\mathrm{sat}}_{11_0} &= \frac{\left(c^{\mathrm{sat}}_{13_0}\right)^2}{c^{\mathrm{sat}}_{33_0}} + 4\left[(1 - \gamma_b)\mu_b + \frac{\alpha_b^2\gamma_b^2\frac{M_b L_b}{C_b}}{1 + Z_N\frac{M_b L_b}{C_b}}\right].\end{aligned} \tag{34}$$

The shear moduli, independent of the presence of fluid, are given, from (23), by

$$c_{55_0} = \frac{1}{\mu_b} + Z_T, \quad c_{66_0} = \mu_b. \tag{35}$$

Eqs (18), (34) and (35) provide explicit analytical expressions for low-frequency elastic moduli of a fractured medium as a function of the properties of the background, fractures, and fluid bulk modulus. Using simple algebra one can show that these equations are exactly equivalent to the equations of the anisotropic Gassmann model for fluid substitution in a porous medium with aligned fractures (Gurevich 2003). This equivalence demonstrates that the model of wave propagation in fractured media proposed in this paper is consistent with the fundamental equations of anisotropic poroelasticity (Gassmann 1951; Brown & Korringa 1975), which are exact in the low-frequency limit. These equations can be used for fluid substitution in fractured porous rocks. More detailed analysis of the effects of background porosity and fluid properties on the low-frequency anisotropy of fractured rocks can be found in Gurevich (2003) and Cardona (2002).

5.2 High frequencies

The results for high frequencies can be obtained by taking the limit $\omega \to \infty$ in eq. (13), keeping in mind we are still restricting ω to be less than ω_B and ω_R. Accordingly, we will use subscript $_{\text{high}}$ instead of subscript $_\infty$, which gives, noting that $\lim_{\omega\to\infty} \cot\sqrt{i\omega B} = -i$,

$$\frac{1}{c^{\text{sat}}_{33_{\text{high}}}} = \left\langle \frac{1}{C} \right\rangle = \frac{h_b}{C_b} + \frac{h_c}{C_c}. \tag{36}$$

This result, that at high frequencies the P-wave elastic modulus is the weighted harmonic average of the saturated moduli of the two media, computed using isotropic Gassmann equations, is to be expected. Indeed, at high frequencies the fluid has no time to move from pores in the background into the fractures, or vice versa. No flow between the media means the interfaces can be considered impermeable, and the whole layered continuum can be considered as a stack of elastic layers. The properties of the stack can be determined by Backus averaging the saturated Gassmann moduli C and μ. Eq. (36) is consistent with this approach.

As $h_c \to 0$, recall that even though L_c is $\mathcal{O}(h_c)$, from eq. (14), the Gassmann modulus C_c remains finite. Thus, the moduli obtained as $h_c \to 0$ are:

$$\frac{1}{c^{\text{sat}}_{33_{\text{high}}}} = \left\langle \frac{1}{C} \right\rangle \to \frac{1}{C_b},$$

$$c^{\text{sat}}_{13_{\text{high}}} = c^{\text{sat}}_{33_{\text{high}}} \left(1 - 2\left\langle \frac{\mu}{C} \right\rangle\right) \to c^{\text{sat}}_{33_{\text{high}}} \left(1 - 2\frac{\mu_b}{C_b}\right) = C_b - 2\mu_b,$$

$$c^{\text{sat}}_{11_{\text{high}}} = \frac{\left(c^{\text{sat}}_{13_{\text{high}}}\right)^2}{c^{\text{sat}}_{33_{\text{high}}}} + 4\left(\langle\mu\rangle - \left\langle \frac{\mu^2}{C} \right\rangle\right) \to \frac{\left(c^{\text{sat}}_{13_{\text{high}}}\right)^2}{c^{\text{sat}}_{33_{\text{high}}}} + 4\mu_b\left(1 - \frac{\mu_b}{C_b}\right) = C_b, \tag{37}$$

which are the same as if there were no fractures. Note that the first and third of eq. (37) show that $c^{\text{sat}}_{33_{\text{high}}} = C_b = c^{\text{sat}}_{11_{\text{high}}}$, that is, at high frequencies, P-wave velocities for waves propagating parallel and perpendicular to layering are equal. This effect is caused by the liquid stiffening the otherwise very compliant fractures, and is a well-known result for elastic fractured (non-porous) media when $Z_N \to 0$ (Hudson 1980; Schoenberg & Douma 1988; Thomsen 1995).

The shear moduli obtained as $h_c \to 0$ are given by

$$c_{55_{\text{high}}} = \frac{1}{\mu_b} + Z_T = c_{55_0}, \qquad c_{66_{\text{high}}} = \mu_b = c_{55_0}, \tag{38}$$

and it is seen that these moduli are unchanged over the entire frequency range.

6 VELOCITY DISPERSION AND ATTENUATION

As can be seen from the previous section, the normal elastic stiffnesses of the fractured medium for low and high frequencies can be very different. For instance, the P-wave modulus along the symmetry axis is given by eq. (18) for low frequencies and is equal to C_b for high frequencies. This means that the stiffness matrix and the corresponding elastic wave velocities are frequency-dependent. By introducing dimensionless fracture weakness δ_N (Hsu & Schoenberg 1993; Bakulin *et al.* 2000) of value between 0 and 1 defined by

$$\delta_N \equiv \frac{Z_N L_b}{1 + Z_N L_b}, \tag{39}$$

the frequency dependence of the P-wave modulus along the symmetry axis, given by eq. (15), can be written in the form

$$\frac{1}{c^{\text{sat}}_{33}} = \frac{1}{C_b} + \frac{\delta_N \left(\frac{\alpha_b M_b}{C_b} - 1\right)^2}{L_b\left[1 - \delta_N + \delta_N \frac{M_b}{C_b}\frac{H}{2}\sqrt{\frac{i\omega}{D_b}}\cot\left(\frac{H}{2}\sqrt{\frac{i\omega}{D_b}}\right)\right]}. \tag{40}$$

Introducing normalized frequency

$$\omega' \equiv \frac{\omega M_b^2 H^2}{4C_b^2 D_b} = \frac{\omega\eta M_b H^2}{4\kappa_b C_b L_b}, \tag{41}$$

we can rewrite eq. (40) as

$$\frac{1}{c^{\text{sat}}_{33}} = \frac{1}{C_b} + \frac{\delta_N \left(\frac{\alpha_b M_b}{C_b} - 1\right)^2}{L_b\left[1 - \delta_N + \delta_N\sqrt{i\omega'}\cot\left(\frac{C_b}{M_b}\sqrt{i\omega'}\right)\right]}. \tag{42}$$

Eq. (42) can be used to evaluate the frequency dependence of the P-wave phase slowness and attenuation for waves propagating perpendicular to the fractures. The P-wave phase slowness is the real part of the complex phase slowness, V_{p3}^{-1} where V_{p3} is given by eq. (16), and the attenuation Q is given by half the ratio of the real part of the complex phase slowness to the imaginary part of the complex phase slowness.

Fig. 2 shows this P-wave speed normalized by the high-frequency velocity $V_p^{\text{high}} = \sqrt{c_{33_{\text{high}}}/\rho}$ (a) and dimensionless attenuation Q^{-1} (b) as a functions of normalized frequency ω' for porous rocks with dry fracture weakness $\delta_N = 0.05$ and different background porosity

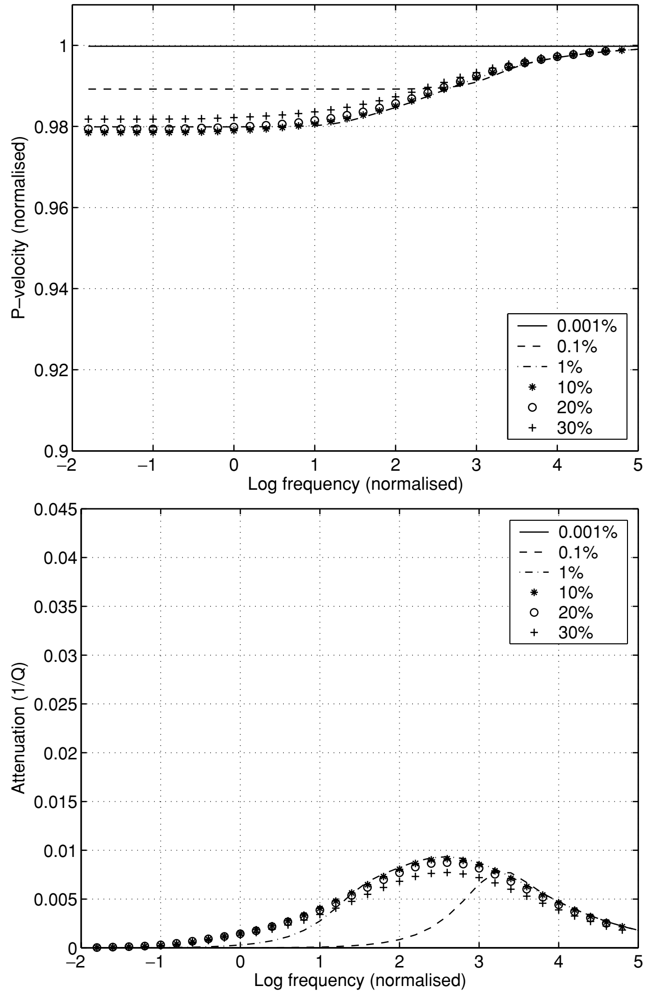

Figure 2. Normalized P-wave speed (a) and inverse quality factor Q^{-1} (b) as functions of normalized frequency for porous rocks with dry fracture weakness $\delta_N = 0.05$ and different background porosity levels.

levels. Fig. 3 shows the results for the same rocks but with higher fracture weakness $\delta_N = 0.2$. The calculations were made for water-saturated sandstone using quartz as the grain material ($K_g = 37$ GPa, $\mu_g = 44$ GPa, $\rho_g = 2.65 \times 10^3$ kg m^{-3}). The dependency of the background dry bulk and shear moduli on porosity was assumed to follow the empirical model of Krief *et al.* (1990)

$$\frac{K_b}{K_g} = \frac{\mu_b}{\mu_g} = (1 - \phi)^{3/(1-\phi)}. \quad (43)$$

Figs 2 and 3 show that velocity dispersion and attenuation have a shape typical for a relaxation phenomenon. For a given δ_N the magnitudes of attenuation and dispersion increase sharply with porosity up to a few per cent porosity, and peak at porosity around 10 per cent. This may look counter-intuitive, as one may expect to find the magnitude of dispersion and attenuation to increase monotonically with porosity. Indeed, it seems logical, as larger porosity allows for larger fluid flow from fractures into pores and vice versa. Thus low-frequency fracture compliance should increase with porosity while the high-frequency fracture compliance should remain unchanged. Indeed, at zero porosity there is no fluid flow between pores and fractures. However, one can also note that when porosity increases, the fluid properties play an increasingly dominant role in the (undrained) elastic moduli of the saturated rock. This effect increases both low- and high-frequency compliances in such a manner that in the limit of 100 per cent porosity they both become equal to the compressibility of the fluid (Gurevich 2003). Therefore, the magnitudes of attenuation and dispersion is zero at both zero and 100 per cent porosity, and thus must have a maximum at some intermediate value of porosity. This value of porosity is controlled by the porosity-velocity dependency for the background, which in our examples is given by the model of Krief *et al.* (1990), eq. (43).

The results for various levels of δ_N are shown in more detail in Figs 4(a) and (b) for typical reservoir background porosity of 20 per cent. As expected, the dispersion and attenuation are proportional to the fracture weakness δ_N. The peak normalized frequency for the attenuation decreases with increasing fracture weakness δ_N. We also note that the dispersion and attenuation are significant over a frequency range that spans at least two orders of magnitude.

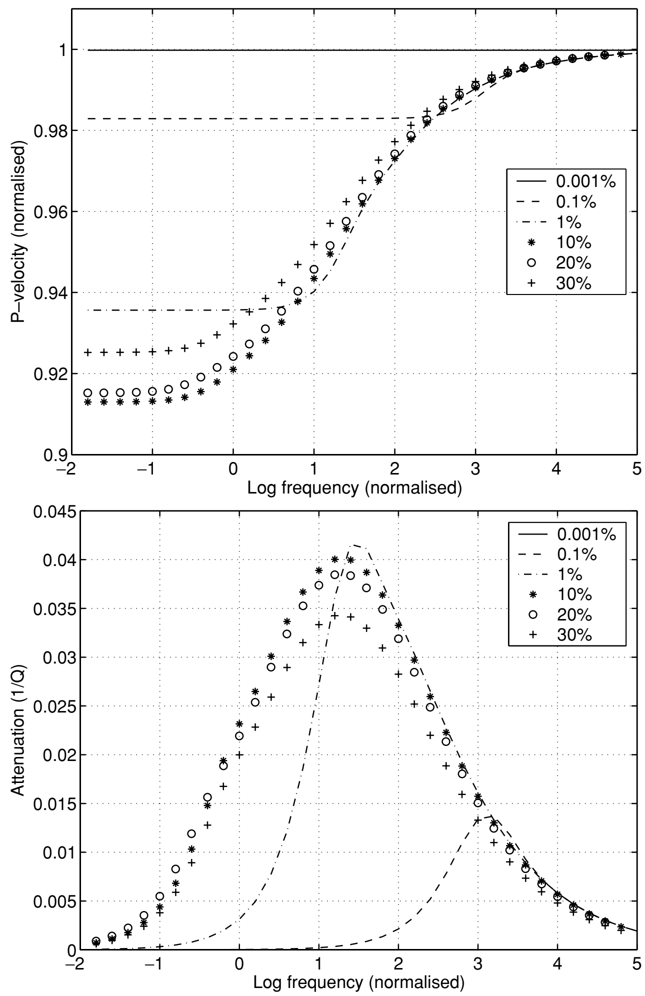

Figure 3. Normalized P-wave speed (a) and inverse quality factor Q^{-1} (b) as functions of normalized frequency for porous rocks with dry fracture weakness $\delta_N = 0.2$ and different background porosity levels.

7 CONCLUSIONS

Fractures in a porous rock can be modelled as very thin and highly porous layers in a porous background. When both pores and fractures are dry, such material is equivalent to a transversely isotropic dry elastic porous material with linear-slip interfaces. When saturated with a liquid this material exhibits significant attenuation and velocity dispersion due to wave-induced fluid flow between pores and fractures. At low frequencies the material properties are equal to those obtained by anisotropic Gassmann theory (Gassmann 1951) applied to a porous material with linear-slip interfaces (Gassmann 1951; Brown & Korringa 1975). At high frequencies the results are equivalent to those for fractures with vanishingly small normal slip in a solid (non-porous) background (Schoenberg & Douma 1988). The characteristic frequency of the attenuation and dispersion depends on the background permeability, fluid viscosity, as well as fracture density and spacing.

The wave-induced fluid flow between pores and fractures considered in this paper has the similar physical nature to so-called squirt flow, which is widely believed to by a major cause of seismic attenuation (Mavko & Nur 1975; O'Connell & Budiansky 1977; Jones 1986). Hence, the present model can be viewed as a new model of squirt-flow attenuation, consistent with Biot's theory of poroelasticity.

Perhaps more accurately, the model of attenuation and dispersion developed in this paper can be viewed as a variant of double porosity models of so-called mesoscopic flow attenuation (Pride *et al.* 2004), a variant designed specifically for open fractures in a poroelastic background. The concept of mesoscopic flow refers to wave-induced flow caused by the presence of mesoscopic heterogeneities, that is, heterogeneities small compared to the wavelength but much larger than the size of individual pores or grains, see e.g. Gurevich & Lopatnikov (1995). Since fractures have zero thickness in our model, the term 'mesoscopic' refers not to fracture opening, but to fracture spacing, which in our model was indeed assumed mesoscopic, that is, much larger than the pore size but much smaller than the wavelength.

The present work is limited to the derivation of the P-wave modulus along the symmetry axis. Derivation of other moduli of the periodically fractured medium would require the solution for the compressional and shear waves of arbitrary incidence in a layered poroelastic medium. This will be done in a separate study.

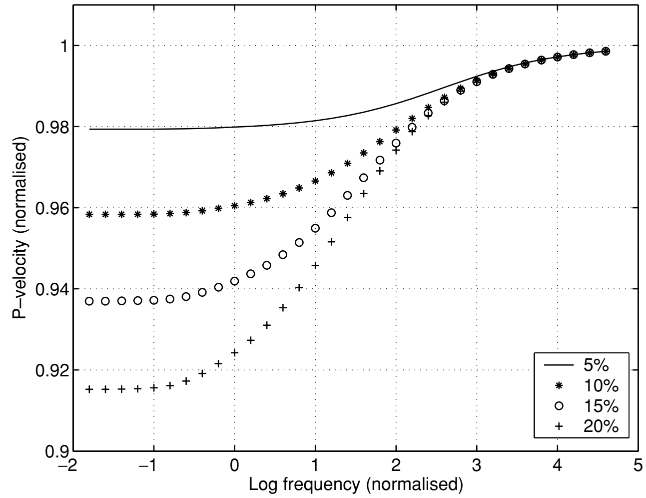

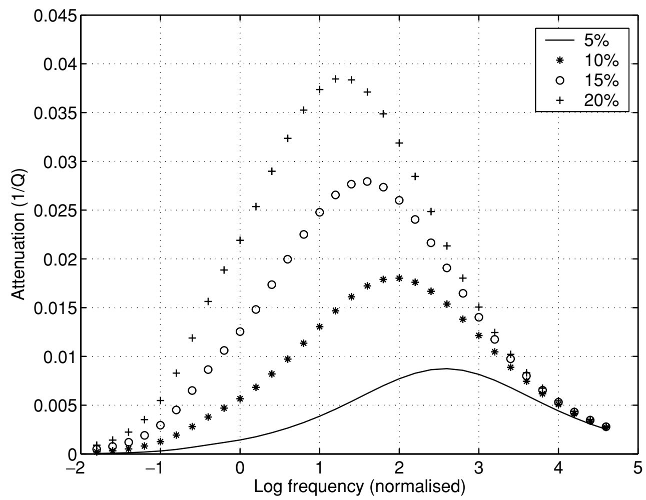

Figure 4. Normalized *P*-wave speed (a) and inverse quality factor Q^{-1} (b) as functions of normalized frequency for porous rocks with background porosity $\phi = 0.2$ and different dry fracture weaknesses.

The present work is also limited by the assumption of periodic distribution of fractures. In reality fractures may be distributed in a random fashion. Sensitivity of our results to the violation of the periodicity assumption will be examined in a numerical study to be published separately.

ACKNOWLEDGMENTS

This work was performed under the financial support of the Centre for Mining Technology and Equipment, CSIRO Petroleum, Centre of Excellence for Exploration and Production Geophysics, and Australian Research Council, Project DP0342998.

REFERENCES

Bakulin, A., Grechka, V. & Tsvankin, I., 2000. Estimation of fracture parameters from reflection seismic data—Part I: HTI model due to a single fracture set, *Geophysics,* **65,** 1788–1802.

Biot, M.A., 1962. Mechanics of deformation and acoustic propagation in porous media, *J. Appl. Phys.,* **33,** 1482–1498.

Brown, R.J.S. & Korringa, J., 1975. On the dependence of the elastic properties of a porous rock on the compressibility of the pore fluid, *Geophysics,* **40,** 608–616.

Cardona, R., 2002. Two theories for fluid substitution in porous rocks with aligned cracks, in *72st Ann. Internat. Mtg., Soc. Expl. Geophys., Expanded Abstracts*, pp. 173–176.

Chapman, M., 2003. Frequency dependent anisotropy due to meso-scale fractures in the presence of equant porosity, *Geophys. Prospect.,* **51,** 369–379.

Deresiewicz, H. & Skalak, R., 1963. On uniqueness in dynamic poroelasicity, *Bull. seism. Soc. Am.,* **53,** 783–788.

Gassmann, F., 1951. Über die elastizität poröser medien, *Viertel. Naturforsch. Ges. Zürich,* **96,** 1–23.

Gelinsky, S. & Shapiro, S.A., 1997. Poroelastic backus averaging for anisotropic layered fluid- and gas-saturated sediments, *Geophysics,* **62,** 1867–1878.

Gurevich, B., 2003. Elastic properties of saturated porous rocks with aligned fractures, *J. appl. Geophys.,* **30,** 203–218.

Gurevich, B. & Lopatnikov, S.L., 1995. Velocity and attenuation of elastic waves in finely layered porous rocks, *Geophys. J. Int.,* **121,** 933–947.

Gurevich, B. & Schoenberg, M., 1999. Interface conditions for Biot's equations of poroelasticity, *J. acoust. Soc. Am.,* **105,** 2585–2589.

Hsu, C. & Schoenberg, M., 1993. Elastic waves through a simulated fractured medium, *Geophysics,* **58,** 964–977.

Hudson, J.A., 1980. Overall properties of a cracked solid., *Math. Proc. Camb. Phil. Soc.,* **88,** 371–384.

Hudson, J.A., Liu, E. & Crampin, S., 1996. The mechanical properties of materials with interconnected cracks and pores., *Geophys. J. Int.,* **124,** 105–112.

Hudson, J., Pointer, T. & Liu, E., 2001. Effective-medium theories for fluid-saturated materials with aligned cracks, *Geophys. Prospect.,* **49,** 509–522.

Jones, T., 1986. Pore fluids and frequency dependent wave propagation in rocks, *Geophysics,* **51,** 1939–1953.

Krief, M., Garat, J., Stellingwerff, J. & Ventre, J., 1990. A petrophysical interpretation using the velocities of P and S waves (Full-Wave Sonic), *The Log Analyst,* **5,** 355–369.

Maultzsch, S., Chapman, M., Liu, E. & Li, X., 2003. Modelling frequency-dependent seismic anisotropy in fluid-saturated rock with aligned fractures: implication of fracture size estimation from anisotropic measurements, *Geophys. Prospect.,* **51,** 381–392.

Mavko, G. & Nur, A., 1975. Melt squirt in the aesthenosphere, *J. geophys. Res.,* **80,** 1444–1448.

Norris, A.N., 1993. Low-frequency dispersion and attenuation in partially saturated rocks, *J. acoust. Soc. Am.,* **94,** 359–370.

O'Connell, R.J. & Budiansky, B., 1977. Viscoelastic properties of fluid-saturated cracked solids, *J. geophys. Res.,* **82,** 5719–5740.

Pride, S., Berryman, J.G. & Harris, J.M., 2004. Seismic attenuation due to wave-induced flow, *J. geophys. Res.,* **109,** No. B1, B01201.

Schoenberg, M., 1980. Elastic wave behavior across linear slip interfaces, *J. acoust. Soc. Am.,* **68,** 1516–1521.

Schoenberg, M. & Douma, J., 1988. Elastic-wave propagation in media with parallel fractures and aligned cracks, *Geophys. Prospect,* **36,** 571–590.

Schoenberg, M. & Sayers, C.M., 1995. Seismic anisotropy of fractured rock, *Geophysics,* **60,** 204–211.

Thomsen, L., 1995. Elastic anisotropy due to aligned cracks in porous rock, *Geophys. Prospec.,* **43,** 805–829.

Tod, S.R., 2001. The effects on seismic waves of interconnected nearly aligned cracks, *Geophys. J. Int.,* **146,** 249–263.

White, J.E., 1983. *Underground Sound: Application of Seismic Waves,* Elsevier, Amsterdam.

White, J.E., Mikhaylova, N.G. & Lyakhovitsky, F.M., 1975. Low-frequency seismic waves in fluid saturated layered rocks, *Izvestija Academy of Sciences USSR, Phys. Solid Earth,* **11**(10), 654–659.

APPENDIX A: DERIVATION OF COMPLEX *P*-WAVE MODULUS FOR A PERIODICALLY LAYERED POROELASTIC MEDIUM

Consider a 1-D periodic medium with spatial period H consisting of alternating uniform layers of saturated poroelastic media 1 and 2 of thicknesses $h_1 H$ and $h_2 H$, $h_1 + h_2 = 1$. Each of the poroelastic layers, assumed to be acoustically described by Biot's equations, is statistically isotropic and homogeneous. For either of the saturated poroelastic media, the relevant (to propagation normal to the layering so that partial derivatives with respect to the x- and y-directions vanish and that σ_{xx} and σ_{yy} need not be considered) constitutive relations and equations of motion are (Biot 1962)

$$\sigma_{zz} = (2\mu + \lambda_s)\frac{\partial u}{\partial z} + \alpha M \frac{\partial w}{\partial z},$$

$$-p = \alpha M \frac{\partial u}{\partial z} + M\frac{\partial w}{\partial z}.$$

$$\frac{\partial \sigma_{zz}}{\partial z} = \frac{\partial^2}{\partial t^2}(\rho u + \rho_f w),$$

$$-\frac{\partial p}{\partial z} = \frac{\partial^2}{\partial t^2}(\rho_f u + m w) + \frac{\eta}{\kappa}\frac{\partial w}{\partial t} = \frac{\partial^2}{\partial t^2}\rho_f u + \frac{\partial}{\partial t}\left(\frac{\eta}{\kappa} + m\frac{\partial}{\partial t}\right) w, \tag{A1}$$

where σ is total normal stress in the z-direction, p is fluid pressure, u is the solid displacement in the z-direction and w is the fluid displacement relative to the solid in the z-direction. The medium parameters are λ_s, the Lamé coefficient of the confined (fluid saturated) porous material, μ, the shear modulus, M the so-called pore space modulus defined by Gassmann's relation (12) and α, the Biot constant (11). δ_{ij} is the Kronecker delta. Here $\rho = (1 - \phi)\rho_g + \phi\rho_f$ is average density of the saturated material and $\eta/\kappa + m\partial/\partial t$ is Biot's visco-dynamic operator. In the frequency domain, this operator becomes

$$-i\omega\tilde{m} \equiv \frac{\eta}{\kappa} - i\omega m \equiv \frac{\eta}{\kappa}\left[1 - i\frac{\omega}{\omega_B}\frac{\phi}{\rho_f} m\right],$$

where $\omega_B \equiv \eta\phi/\kappa\rho_f$ is the Biot frequency. For frequencies much smaller than ω_B, the operator in the frequency domain becomes just the viscous operator, η/κ. This is the frequency regime in which we are deriving the P-wave moduli for the two-layer periodic system. In any event, this viscous flow term is responsible for the dissipation.

Letting pressure, stress and displacements be harmonic functions of time, that is, with time dependence of the form $\exp(-i\omega t)$, eq. (A1) can be written, in the frequency domain, as four differential equation on $\dot{u}$, $\dot{w}$, σ_{zz} and p. Then, after some matrix manipulation, these equations can be written as a first order system of equations in standard matrix form

$$\frac{\partial}{\partial z}\mathbf{b}(z) = -i\omega\,\mathbf{Q}\,\mathbf{b}(z),$$

$$\mathbf{b} \equiv \begin{bmatrix} \dot{u} \\ \dot{w} \\ \sigma_{zz} \\ -p \end{bmatrix} \quad \text{and} \quad \mathbf{Q} \equiv \begin{bmatrix} 0 & 0 & 1/L & -\alpha/L \\ 0 & 0 & -\alpha/L & C/ML \\ \rho & \rho_f & 0 & 0 \\ \rho_f & i\frac{\eta}{\omega\kappa} + m & 0 & 0 \end{bmatrix}. \tag{A2}$$

Here, $C \equiv 2\mu + \lambda_s$ and $L \equiv C - \alpha^2 M$. Open pore conditions ensure the continuity of the four-vector $\mathbf{b}$ across $z = $ const interfaces, (Deresiewicz & Skalak 1963; Gurevich & Schoenberg 1999).

The solution of eq. (A2) within a single homogeneous layer is,

$$\mathbf{b}(z) = \underbrace{e^{-i\omega(z-z_0)\mathbf{Q}}}_{\mathbf{P}(z-z_0)}\,\mathbf{b}(z_0) \equiv \sum_{n=0}^{\infty} \frac{[-i\omega(z-z_0)]^n}{n!}\mathbf{Q}^n\,\mathbf{b}(z_0) \equiv \mathbf{A}e^{-i\omega(z-z_0)\boldsymbol{\Lambda}}\mathbf{A}^{-1}\,\mathbf{b}(z_0). \tag{A3}$$

$\mathbf{P}(z-z_0)$ is called propagator matrix. $\boldsymbol{\Lambda}$ is the diagonal matrix of eigenvalues of $\mathbf{Q}$; $\mathbf{A}$ is the matrix whose columns are eigenvectors of $\mathbf{Q}$, the kth column being the eigenvector associated with the kth eigenvalue. The eigenvalues of $\mathbf{Q}$ are the roots of a quartic equation that is actually a quadratic equation on the squares of the roots:

$$\lambda^4 - \frac{1}{L}\left[\frac{\left[i\frac{\eta}{\omega\kappa}+m\right]C}{M} + \rho - 2\alpha\rho_f\right]\lambda^2 + \frac{\rho\left[i\frac{\eta}{\omega\kappa}+m\right]-\rho_f^2}{LM} = 0. \tag{A4}$$

The eigenvalues are the slownesses of four vertically propagating compressional waves (displacements in the direction of propagation), two up and two down. To see which pair of roots corresponds to which pair of down and up-going waves, these roots are evaluated as $\omega \to 0$. In this limit, $\lambda_+^2 \to i\eta C/\omega\,\kappa ML \equiv i/\omega D$ and $\lambda_-^2 \to \rho/C$ so the '+' root is the square of the diffusive (d) wave (low-frequency Biot slow wave) slowness, and the '−' root is the square of the usual fast compressional (p) wave slowness.

For a stack of n spatial periods H of two layers each, of thicknesses h_1H and h_2H (h_1 and h_2 are the relative thicknesses), and letting reference level $z_0 = 0$, the solution, from eq. (A3), becomes

$$\begin{aligned}\mathbf{b}(nH) &= [\exp(-i\omega h_2 H\mathbf{Q}_2)\exp(-i\omega h_1 H\mathbf{Q}_1)]^n\,\mathbf{b}(0)\\ &\equiv \Big[\underbrace{\mathbf{A}_2\exp(-i\omega h_2 H\boldsymbol{\Lambda}_2)\mathbf{A}_2^{-1}\mathbf{A}_1\exp(-i\omega h_1 H\boldsymbol{\Lambda}_1)\mathbf{A}_1^{-1}}_{\mathbf{P}(H)}\Big]^n\mathbf{b}(0).\end{aligned} \tag{A5}$$

Note that the exponent n cannot be moved inside the brackets as, in general, matrix multiplication is not commutative. This procedure can be used to give the exact propagator matrix through a single period, $\mathbf{P}(H)$. However, for low-frequency propagation relative to each of the Biot media,

$$\mathbf{P}(H) \sim \mathbf{P}(H)|_{\lambda_+\to\sqrt{i/\omega D},\,\lambda_-\to\sqrt{\rho/C}} \equiv \mathbf{P_0}(H). \tag{A6}$$

For wavelengths of the incident wave much longer than the spatial period of stratification, effective medium theory can be used. Our aim is to find effective slownesses of the waves propagating in the equivalent medium, that is, eigenvalues of an effective system matrix $\mathbf{Q}^*$, so that we can write,

$$\mathbf{P_0}(H) \equiv \exp(-i\omega H\mathbf{Q}^*) = \mathbf{A}^*\exp(-i\omega H\boldsymbol{\Lambda}^*)(\mathbf{A}^*)^{-1}, \tag{A7}$$

where $\boldsymbol{\Lambda}^*$ is diagonal matrix of eigenvalues of the equivalent medium, its possible vertical slownesses, and $\mathbf{A}^*$ is the matrix of corresponding eigenvectors. The eigenvalues are the roots of the characteristic equation

$$\det[\mathbf{P_0} - \lambda\mathbf{I}] \equiv \lambda^4 - \mathrm{Tr}_{\mathbf{P_0}}(\omega)\lambda^3 + \mathrm{II}_{\mathbf{P_0}}(\omega)\lambda^2 - \mathrm{III}_{\mathbf{P_0}}(\omega)\lambda + 1 = 0.$$

The constant term is unity since the determinant of any propagator matrix is 1. $\mathrm{Tr}_{\mathbf{P_0}}$ denotes the trace, $\mathrm{II}_{\mathbf{P_0}}$ the second invariant and $\mathrm{III}_{\mathbf{P_0}}$ the third invariant of the 4×4 matrix $\mathbf{P}_0$. Furthermore, because eigenvalues of $\exp(-i\omega H\mathbf{Q}^*)$ represent slownesses of fast and slow compressional waves in an equivalent medium, they appear in pairs as follows: $\exp(\pm\, i\omega H\lambda_p^*)$ and $\exp(\pm\, i\omega H\lambda_d^*)$. That $\mathrm{Tr}_{\mathbf{P_0}}$ is the sum of the roots, $\mathrm{II}_{\mathbf{P_0}}$ is the sum of two products of roots and $\mathrm{III}_{\mathbf{P_0}}$ is the sum of three products of roots, implies that

$$\mathrm{III}_{\mathbf{P_0}} = \mathrm{Tr}_{\mathbf{P_0}} = 2\left[\cos\omega H\lambda_p^* + \cos\omega H\lambda_d^*\right], \quad \mathrm{II}_{\mathbf{P_0}} = 2\left[1 + 2\cos\omega H\lambda_p^*\,\cos\omega H\lambda_d^*\right]. \tag{A8}$$

The solution of these two non-linear simultaneous equations in $\cos\omega H\lambda_p^*$ and $\cos\omega H\lambda_d^*$ is,

$$\cos\omega H\lambda^* = \frac{1}{4}\left[\mathrm{Tr}_{\mathbf{P_0}} \pm \sqrt{\mathrm{Tr}_{\mathbf{P_0}}^2 - 4\,\mathrm{II}_{\mathbf{P_0}} + 8}\right], \tag{A9}$$

but note that since period H is assumed small compared to the wavelength of the fast wave, $\omega H\lambda_p^* \ll 1$ and thus $\cos\omega H\lambda_p^* \sim 1$. This implies, from eq. (8), that

$$\mathrm{Tr}_{\mathbf{P_0}} \sim 2[1 + \cos\omega H\lambda_d^*], \quad \mathrm{II}_{\mathbf{P_0}} \sim 2[1 + 2\cos\omega H\lambda_d^*],$$

and, subsequently, that

$$\sqrt{\mathrm{Tr}_{\mathbf{P_0}}^2 - 4\mathrm{II}_{\mathbf{P_0}} + 8} \sim \sqrt{4[1+\cos\omega H\lambda_d^*]^2 - 8[1 + 2\cos\omega H\lambda_d^*] + 8} = 2[1 - \cos\omega H\lambda_d^*].$$

Thus,

$$\frac{1}{4}\left[\mathrm{Tr}_{\mathbf{P_0}} + \sqrt{\mathrm{Tr}_{\mathbf{P_0}}^2 - 4\,\mathrm{II}_{\mathbf{P_0}} + 8}\right] \sim 1, \quad \frac{1}{4}\left[\mathrm{Tr}_{\mathbf{P_0}} - \sqrt{\mathrm{Tr}_{\mathbf{P_0}}^2 - 4\,\mathrm{II}_{\mathbf{P_0}} + 8}\right] \sim \cos\omega H\lambda_d^*,$$

and clearly the + sign corresponds to the fast P wave, the − sign to the slow diffusive wave. As our aim is an expression for the modulus corresponding to the low frequency fast P wave, we have

$$\cos\omega H\lambda_p^* = \frac{1}{4}\left[\mathrm{Tr}_{\mathbf{P_0}} + \sqrt{\mathrm{Tr}_{\mathbf{P_0}}^2 - 4\,\mathrm{II}_{\mathbf{P_0}} + 8}\right]. \tag{A10}$$

$\mathrm{Tr}_{\mathbf{P_0}}$ and $\mathrm{II}_{\mathbf{P}_0}$ are known functions of frequency as well as of the material properties and thicknesses of the two layers. More precisely, from the structure of $\mathbf{P_0}$ in eq. (A5), $\mathrm{Tr}_{\mathbf{P_0}}$ and $\mathrm{II}_{\mathbf{P_0}}$ are, respectively, known quadratic and fourth-power homogeneous polynomials in fast P wave terms, $\sin \omega h_j H\sqrt{\rho_j/C_j}$, $\cos \omega h_j H\sqrt{\rho_j/C_j}$, and slow diffusive wave terms,

$$\sin \omega h_j H\sqrt{i/\omega D_j} = \sin h_j H\sqrt{i\omega/D_j}, \quad \cos \omega h_j H\sqrt{i/\omega D_j} = \cos h_j H\sqrt{i\omega/D_j},$$

$j = 1, 2.$

However, at low (but not zero) frequency, to get a dispersion relation for the fast P wave, we use the fact that the $\omega h_j H\sqrt{\rho_j/C_j}$, $j = 1, 2$, are also small. To account for this, a small parameter ϵ is introduced through the substitution

$$\omega h_j H\sqrt{\rho_j/C_j} \to \epsilon\widetilde{\lambda}_{pj}\ , \quad j = 1, 2.$$

Since $\mathrm{Tr}_{\mathbf{P}_0}(\omega)$ and $\mathrm{II}_{\mathbf{P}_0}(\omega)$ depend on the P-wave slownesses only through cosines and sines, and we are interested in expansions of $\mathrm{Tr}_{\mathbf{P_0}}$ and $\mathrm{II}_{\mathbf{P_0}}$ only to order ϵ^2, we substitute $\cos \omega h_j H\sqrt{\rho_j/C_j} \sim 1 - (\epsilon^2\widetilde{\lambda}^2_{pj})/2$ and $\sin \omega h_j H\sqrt{\rho_j/C_j} \sim \epsilon\widetilde{\lambda}_{pj}$, $j = 1, 2$, into the expressions for $\mathrm{Tr}_{\mathbf{P}}$ and $\mathrm{II}_{\mathbf{P}}$, giving the formal expansions,

$$\mathrm{Tr}_{\mathbf{P}} \sim 2\left[a_0 + a_1\epsilon + a_2\epsilon^2\right], \qquad \mathrm{II}_{\mathbf{P}} \sim 2\left[b_0 + b_1\epsilon + b_2\epsilon^2\right].$$

Note that a_0 and b_0 are independent of the $\widetilde{\lambda}_{pj}$, a_1 and b_1 are linear functions of the $\widetilde{\lambda}_{pj}$, and a_2 and b_2 are quadratic functions of the $\widetilde{\lambda}_{pj}$. Substituting these expansions into eq. (A10), and expanding the right-hand side in powers of ϵ gives,

$$\begin{aligned}\cos \omega H\lambda^*_p &= \frac{1}{2}\Big[a_0 + a_1\epsilon + a_2\epsilon^2 + \sqrt{a_0^2 - 2b_0 + 2 + 2(a_1a_0 - b_1)\epsilon + \left[2a_2a_0 + a_1^2 - 2b_2\right]\epsilon^2}\ \Big] \\ &= \frac{1}{2}\left\{a_0 + \sqrt{a_0^2 - 2b_0 + 2} + \left(a_1 + \frac{a_1a_0 - b_1}{\sqrt{a_0^2 - 2b_0 + 2}}\right)\epsilon\right. \\ &\quad \left. + \left(a_2 + \frac{2a_2a_0 + a_1^2 - 2b_2}{2\sqrt{a_0^2 - 2b_0 + 2}} - \frac{(a_1a_0 - b_1)^2}{2\sqrt{(a_0^2 - 2b_0 + 2)^3}}\right)\epsilon^2\right\}. \end{aligned} \tag{A11}$$

Finding the coefficients of ϵ and ϵ^2 in the expansions for $\mathrm{Tr}_{\mathbf{P}}$ and $\mathrm{II}_{\mathbf{P}}$ is complicated and substituting them into the right hand side of eq. (A11) is very cumbersome but the procedure is basically straight forward. Then, after expressing $\cos h_j H\sqrt{i\omega/D_j}$ and $\sin h_j H\sqrt{i\omega/D_j}$, $j = 1, 2$, in terms of cotangents of half arguments, that is, using the identities,

$$\sin\theta = \frac{2\cot(\theta/2)}{\cot^2(\theta/2) + 1}, \quad \cos\theta = \frac{\cot^2(\theta/2) - 1}{\cot^2(\theta/2) + 1},$$

and then replacing the $\epsilon\widetilde{\lambda}_{pj}$ with the original fast P wave arguments, $\omega h_j H\sqrt{\rho_j/C_j}$, one obtains,

$$\cos \omega H\lambda^*_p = 1 - \frac{\omega^2 H^2\langle\rho\rangle}{2}\left[\left\langle\frac{1}{C}\right\rangle + \frac{B(\omega)}{H}\right], \tag{A12}$$

$$B(\omega) = \frac{2}{\sqrt{i\omega}\,\eta}\ \frac{\left(\frac{\alpha_1 M_1}{C_1} - \frac{\alpha_2 M_2}{C_2}\right)^2}{\frac{\sqrt{D_1}}{\kappa_1}\cot\left(\frac{h_1 H}{2}\sqrt{\frac{i\omega}{D_1}}\right) + \frac{\sqrt{D_2}}{\kappa_2}\cot\left(\frac{h_2 H}{2}\sqrt{\frac{i\omega}{D_2}}\right)}, \tag{A13}$$

where $\langle\rho\rangle \equiv h_1\,\rho_1 + h_2\,\rho_2$ is the thickness averaged density, $\langle 1/C\rangle = h_1/C_1 + h_2/C_2$ is the thickness averaged inverse of P-wave modulus, and

$$D_j = \frac{\kappa_j M_j L_j}{\eta C_j}\ ,\ \ j = 1, 2.$$

For sufficiently low frequencies, this result can be written,

$$(\lambda^*_p)^2 = \langle\rho\rangle\left[\left\langle\frac{1}{C}\right\rangle + \frac{B\,(\omega)}{H}\right] \equiv \frac{\langle\rho\rangle}{C^*}, \tag{A14}$$

and substituting $B(\omega)$ from eq. (A13) gives a value for C^* in agreement with eq. (13).